High performance ultrafine-grained Ti-Fe-based alloys with multiple length-scale phases

Lai-Chang Zhang*

School of Mechanical and Chemical Engineering, The University of Western Australia, 35 Stirling Highway, Crawley, Perth, WA 6009, Australia

(Received January, 7, 2012, Revised February 10, 2012, Accepted February 14, 2012)

Abstract. In order to simultaneously enhance the strength and plasticity in nanostructured / ultrafine-grained alloys, a strategy of introducing multiple length scales into microstructure (or called bimodal composite microstructure) has been developed recently. This paper presents a brief overview of the alloy developement and the mechanical behavior of ultrafine-grained Ti-Fe-based alloys with different length-scale phases, i.e., micrometer-sized primary phases (dendrites or eutectic) embedded in an ultrafine-grained eutectic matrix. These ultrafine-grained titanium bimodal composites could be directly obtained through a simple single-step solidification process. The as-prepared composites exhibit superior mechanical properties, including high strength of 2000-2700 MPa, large plasticity up to 15-20% and high specific strength. Plastic deformation of the ultrafine-grained titanium bimodal composites occurs through a combination of dislocation-based slip in the nano-/ultrafine scale matrix and constraint multiple shear banding around the micrometer-sized primary phase. The microstructural charactersitcs associated to the mechanical behaivor have been detailed discussed.

Keywords: titanium alloy; bimodal composite; multiple length scales; ultrafine-grained; mechanical behavior; microstructure

1. Introduction

Nanostructured and ultrafine-grained metals and alloys have been attracted considerable interest due to their excellent mechanical properties. The nanostructured / ultrafine-grained metallic materials have a strength up to several times compared with their conventional coarse-grained counterparts. For example, nanostructured and ultrafine-grained pure copper has a yield strength of 400-900 MPa and 200 MPa, respectively (Ma 2003b), which are several times up to an order of magnitude higher than that of the conventional coarse-grained copper. The superior high strength creates the possibility of weight and energy saving. Therefore, such fine-grained metallic materials are expected to have many potential applications. Although these fine-grained materials offer extraordinary properties, most these super-strong nanostructured / ultrafine-grained materials generally have a very limited plasticity. The poor plasticity makes them unusable in load-bearing applications. The major limitations of plasticity for the fine-grained metallic materials have been identified (Koch 2003, Ma 2003b) as artefacts from processing, force instability, and crack nucleation

*Corresponding author, Assistant Professor, E-mails: lczhangimr@gmail.com; laichang.zhang@uwa.edu.au

and propagation instability. Therefore, considerable efforts are being made to enhance room-temperature plasticity as well as to maintain a high strength in the development of nanostructured / ultrafine-grained metallic materials. For this purpose, several strategies have been developed to attain a good combination with enhanced plasticity and high strength (Ma 2003b, 2006). Nanostructured / ultrafine-grained metallic materials are usually made into bulky form through multiple processing steps, e.g., via powder metallurgy of nanostructured / ultrafine-grained powders, or crystallization from amorphous precursors, or by employing techniques that are not easily commercially viable, such as severe plastic deformation techniques (Sun *et al.* 2006).

Recent investigations have highlighted that introducing multiple length-scale phases in microstructure is effective to simultaneously achieve high strength and large plasticity in nanostructured / ultrafine-grained metallic materials (Wang *et al.* 2002). Bulk nanostructured / ultrafine-grained materials with multiple length-scale phases could be obtained by easy manufacturing process (i.e., simple single step casting) (He *et al.* 2003, Louzguine *et al.* 2004, Das *et al.* 2005, Louzguine-Luzgin *et al.* 2005, Zhang *et al.* 2007a, Zhang *et al.* 2007b, Han *et al.* 2008, Park *et al.* 2009, Misra *et al.* 2010b, Zhang *et al.* 2010). The as-cast bulk nanostructured / ultrafine-grained materials with multiple length-scale phases exhibit not only high strength exceeding 2000 MPa, like bulk metallic glasses (Johnson 1999, Inoue 2000), but also large plasticity of 15-20%, which is much larger than the plasticity of the majority bulk nanostructured / ultrafine-grained materials with uniform grain size distribution or bulk metallic glasses (Zhang *et al.* 2007b, Hofmann *et al.* 2008, Zhang *et al.* 2011). The appealing properties can be ascribed to their multiple length-scale microstructure with micrometer-sized primary phases (dendrites or eutectic) embedded in the nanostructured / ultrafine-grained eutectic matrix. The high strength is provided by the nanostructured / ultrafine-grained eutectic matrix, whereas the enhanced plasticity stems from the heterogeneous microstructure (or multiple length-scale hierarchical structure) that suppresses deformation instability (Ma 2003a). Thus, the materials with multiple length-scale phases exhibit unusual deformation mechanisms similar to the ductile-phase toughening brittle materials. Coarse-grained bands tend to deform locally at stress concentrations, arresting cracks by local blunting and resisting crack growth by bridging of crack wakes. In other word, plastic deformation of these bimodal composite materials occurs through a combination of dislocation-based slip in the fine-grained matrix and constraint multiple shear banding around the dendrites-eutectic interface (Louzguine-Luzgin *et al.* 2005, Sun *et al.* 2006, Zhang *et al.* 2007a, Han *et al.* 2008, Park *et al.* 2009). The deformation mechanisms can be altered by tailoring morphology and dispersion of coarse-grained phase, as well as interface properties. With the promise of superior mechanical properties, it is likely that many structural applications should open up for nanostructured / ultrafine-grained metallic materials.

The combination of low density (4500 kg/m^3), excellent mechanical properties (strength ~1000 MPa, ductility ~10%) and good corrosion resistance makes titanium and its alloys one of the best engineering materials. Very recently, bulky nanostructured / ultrafine-grained titanium based bimodal alloys with heterogeneities of length scale have received a lot of attention, as the formation of bimodal composite microstructure seems an effective approach for novel microstructure design to enhance the plasticity of high-strength titanium alloys (He *et al.* 2003, Louzguine *et al.* 2004, Louzguine-Luzgin *et al.* 2005, Zhang *et al.* 2007a, Zhang *et al.* 2007b, Han *et al.* 2008, Park *et al.* 2009, Misra *et al.* 2010b, Zhang *et al.* 2010). In particular, these nanostructured / ultrafine-grained titanium bimodal composites have been highlighted for practical applications due to their easy and simple processing (*via* casting). These as-prepared titanium alloys exhibit high strength of 2000-2700 MPa and large plasticity up to 15-20%. For example, $Ti_{60}Cu_{14}Ni_{22}Sn_4Nb_{10}$ rods composed of micrometer-sized β-Ti dendrites embedded in a nanostructured matrix exhibits a high compressive strength of 2400 MPa and 14.5% plastic strain (He *et al.* 2003). More recently, in a much cheaper Ti-Fe alloy, the hypereutectic $Ti_{65}Fe_{35}$ alloy consisting of β-Ti and FeTi phases exhibit better compressive mechanical properties (strength ~2200 MPa, plasticity ~6.7%) than the hypoeutectic and eutectic alloys (Louzguine *et al.* 2004).

Due to low alloy cost and excellent mechanical properties, considerable studies have been being conducted on the alloy design and manipulation of microstructural heterogeneities in Ti-Fe alloys with aim to further achieve a better combination of high strength and large plasticity. This paper presents a brief overview of the alloy development in Ti-Fe binary hypereutectic, eutectic and hypoeutectic alloys via micro-alloying and the mechanical behavior of the ultrafine-grained Ti-Fe-based alloys with different length-scale phases.

2. Alloy development in Ti-Fe-based alloys

2.1 Ti-Fe binary alloys

Compared with the formation of Ti-based bimodal composites from bulk glass-forming alloys (He *et al.* 2003, Louzguine *et al.* 2004) obtained the bimodal microstructure in a much cheaper binary Ti-Fe alloy system only by arc melting procedure. The microstructure of the hypereutectic, eutectic or hypoeutectic Ti-Fe alloys produced by arc-melting consists of b.c.c. Pm3m TiFe and b.c.c. $Im\bar{3}m$ β-Ti solid solution phase. Most Ti-Fe binary alloys exhibit an excellent combination with high strength and large plasticity, as shown in Fig. 1. Compared with the hypoeutectic and eutectic alloys, the hypereutectic $Ti_{65}Fe_{35}$ alloy with micrometer-sized rounded FeTi primary dendrites dispersed in an ultrafine-grained (β-Ti + FeTi) eutectic matrix exhibits the best mechanical properties (strength ~2200 MPa, plasticity ~6.7%) under compression. Studies on the deformation behavior of the $Ti_{65}Fe_{35}$ bimodal composite demonstrated that the propagation of large cracks is blocked by primary FeTi dendrites and the fine eutectic FeTi crystals are cut by micro-cracks (Louzguine *et al.* 2004). Therefore, the multiple length-scale phases in $Ti_{65}Fe_{35}$ alloy make the alloy

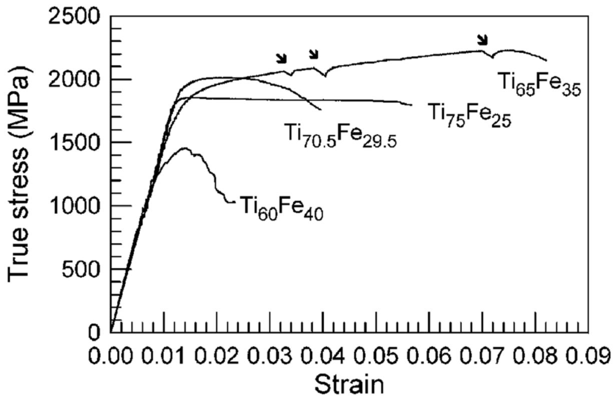

Fig. 1 The strain–stress curves of the $Ti_{100x}Fe_x$ alloys under compressive test, showing the best mechanical properties in the hypereutectic alloys. Reprinted from (Louzguine *et al.* 2004)

Table 1 Mechanical properties at room temperature for some Ti-Fe-based ultrafine-grained bimodal composites (in at.%) prepared by melt casting. σ_y: 0.2% strain offset yield stress, σ_{max}: ultimate stress; ε_p: plastic strain

Alloy	σ_y (MPa)	σ_{max} (MPa)	ε_p (%)	Reference
Hypereutectic				
$Ti_{65}Fe_{35}$*	1800	2200	6.7	(Louzguine-Luzgin *et al.* 2005)
$Ti_{65}Fe_{35}$	1722	2365	7.4	(Zhang *et al.* 2007a)
$(Ti_{0.655}Fe_{0.35})_{97.5}Sn_{2.5}$	1478	2652	12.5	(Zhang *et al.* 2007a)
$(Ti_{0.655}Fe_{0.35})_{95}Sn_5$	1267	2345	10.0	(Zhang *et al.* 2007a)
$Ti_{60}Fe_{20}Co_{20}$*	1510	2100	15	(Louzguine-Luzgin *et al.* 2005)
$(Ti_{0.655}Fe_{0.35})_{98}Ga_2$	2042	2769	6.5	(Misra *et al.* 2010b)
$(Ti_{0.655}Fe_{0.35})_{96}Ga_4$	1953	2472	4.9	(Misra *et al.* 2010b)
$(Ti_{0.655}Fe_{0.35})_{97}Nb_3$	1910	2160	6	(Park *et al.* 2009)
$(Ti_{0.655}Fe_{0.35})_{95}Nb_5$	1964	2390	13	(Park *et al.* 2009)
$(Ti_{0.705}Fe_{0.295})_{95}Sn_5$	2205	2266	1.7	(Han *et al.* 2008)
$(Ti_{0.705}Fe_{0.295})_{93}Sn_7$	1651	1961	6.2	(Han *et al.* 2008)
$(Ti_{0.705}Fe_{0.295})_{91}Sn_9$	1304	2261	15.7	(Han *et al.* 2008)
Hypoeutectic				
$Ti_{72}Fe_{28}$	2028	2627	7.5	(Zhang *et al.* 2007b)
$(Ti_{0.72}Fe_{0.28})_{98}Ta_2$	2300	2560	1.0	(Zhang *et al.* 2007b)
$(Ti_{0.72}Fe_{0.28})_{96}Ta_4$	2215	2531	5.0	(Zhang *et al.* 2007b)
Pseudo-eutectic				
$(Ti_{0.705}Fe_{0.295})_{96.15}Sn_{3.85}$	1794	1974	9.6	(Das *et al.* 2005)
$(Ti_{0.655}Fe_{0.345})_{93}Nb_7$	2182	2574	12	(Park *et al.* 2009)
$Ti_{63.5}Fe_{30.5}Sn_6$	1766	2164	8.4	(Song *et al.* 2011)

* prepared by arc melting

under deformation to act as a composite material consisting of the hard primary FeTi dendrites embedded in a relatively ductile eutectic matrix, resulting in high strength and large plasticity.

In order to further enhance the strength and plasticity in Ti-Fe binary alloys, extensive studies have been being conducted on Ti-Fe binary alloys to tailor multiple length-scale microstructure by micro-alloying (such as Co, Sn, Ta, Nb, Ga, In, etc.) into Ti-Fe binary alloys (Louzguine *et al.* 2004, Das *et al.* 2005, Louzguine-Luzgin *et al.* 2005, Louzguina-Luzgina *et al.* 2006, Zhang *et al.* 2007a, Zhang *et al.* 2007b, Han *et al.* 2008, Park *et al.* 2009, Misra *et al.* 2010b, Zhang *et al.* 2010). It has been revealed that microstructural modification and optimization by additional micro-alloying elements are the key factors to tune the mechanical properties in the ultrafine-grained Ti-Fe alloys. The addition of Sn, Co, Cu and Nb enhanced the plasticity (Louzguine-Luzgin *et al.* 2005, Zhang *et al.* 2007a, Misra *et al.* 2010b) whilst B, Cr, Si, Mn and Ni significantly decreases the plasticity of the $Ti_{65}Fe_{35}$ alloy (Louzguina *et al.* 2005). Interestingly, cheap element Sn could simultaneously improve strength and enhance plasticity of hypereutectic $Ti_{65}Fe_{35}$ and eutectic $Ti_{70.5}Fe_{29.5}$ alloys. For example, ultrafine-grained $Ti_{63.375}Fe_{34.125}Sn_{2.5}$ bimodal composite exhibits a ultimate strength of 2650 MPa and a large plasticity of 12.5% (Zhang *et al.* 2007a) and ultrafine-grained $Ti_{67.79}Fe_{28.36}Sn_{3.85}$ eutectics has high ultimate strength of 1900 MPa and enhanced plasticity of 9.6% (Das *et al.* 2005). The strength and plasticity of the ultrafine-grained titanium alloys with multiple length-scale phases are strongly related to the occurrence of the slip / shear bands in the ultrafine eutectic matrix and the propagation of primary and secondary shear bands in the micron-scale primary phase. It is apparent that controlling the length scale and the intrinsic properties of the constituent phases can enhance the plasticity of high-strength ultrafine-grained titanium alloys. Table 1 gives some examples of the influence of micro-alloying elements on the microstructure and mechanical properties of hypereutectic (e.g., $Ti_{65}Fe_{35}$), eutectic ($Ti_{70.5}Fe_{29.5}$) and hypoeutectic (e.g., $Ti_{72}Fe_{28}$) Ti-Fe alloys. Compared to the ultrafine-grained matrix – dendrite titanium alloys, the mechanical properties of the Ti-Fe-based ultrafine-grained alloys is not sensitive to the solidification process, but to the micro-alloying elements and their concentrations. For example, the $Ti_{65}Fe_{35}$ alloys prepared by arc-melting (Louzguine *et al.* 2004) and by chill-casting (Zhang *et al.* 2007a) have comparable mechanical properties (Table 1). The as-cast eutectic (Das *et al.* 2005, Han *et al.* 2008) and hypoeutectic (Zhang *et al.* 2007b) Fe-Ti bimodal composites also exhibit a high yield strength exceeding 2000 MPa, a high fracture strength over 2500 MPa, and a large plasticity over 5%. Compared with the hypereutectic microstructure, phase transformation in eutectic $Ti_{70.5}Fe_{29.5}$ alloy is somewhat difficult to control when alloyed with additional element.

2.2 Hypereutectic bimodal composites

Due to its excellent mechanical properties, extensive work has investigated the effect of alloying elements on microstructure and mechanical properties of the hypereutectic $Ti_{65}Fe_{35}$ alloy. Louzguine *et al.* (2005) have carried out a thorough investigation of the microstructure, mechanical properties and deformation behavior of the Ti-Fe-Co alloys containing 24-46 at.% (Fe + Co) content. The alloy composition, phase constituents and mechanical properties of the studied alloys were listed in Table 2. The studied Ti-Fe-Co alloys are either hypereutectic (e.g., $Ti_{70}Fe_{20}Co_{10}$, $Ti_{60}Fe_{20}Co_{20}$) or hypoeutectic (e.g., $Ti_{76}Fe_{12}Co_{12}$). The primary phase in hypoeutectic and hypereutectic alloys is β-Ti solid solution and rounded cP2 (Fe, Co)Ti dendrites phase, respectively, and the matrix is (β-Ti + (Fe, Co)Ti) eutectic. The average grain size of the primary phases is 10-20 μm depending on alloy composition, while the diameter or lamellar spacing of eutectic is in submicron. As seen from Table 2, the hypereutectic Ti-Fe-Co alloys exhibit high mechanical strength exceeding 2000 MPa and plasticity up to 16%. Investigation of the Ti-Fe-Co alloys with equiatomic Fe and Co concentration (Louzguine-Luzgin *et al.* 2007) showed that the maximums in strength and plasticity values in the alloys are also located in a hypereutectic composition area. The high strength results from the high Fe and Co contents in the supersaturated β-Ti solid solution (solid solution hardening effect) and high hardness of the (Fe, Co)Ti intermetallic compound having a rounded dendritic morphology. Most of the Ti-Fe-Co hypereutectic alloys also show a strong tendency for strain-hardening. The formation of Ti_2Co phase seems to cause the embrittlement of the Ti-Fe-Co alloys. Among all the studied alloys, the hypereutectic $Ti_{70}Fe_{15}Co_{15}$ alloy shows the best mechanical properties, i.e., strength of 2350 MPa and plasticity of about 16%.

The influence of additional alloying elements (V, Ni, Cu, Sn, Si, B) has also been studied on the

Table 2 Alloy composition, mechanical properties, density (ρ) and phase constituents of the Ti-Fe-Co alloys. *HV* is Vickers microhardness, σ_y: 0.2% strain offset yield stress, σ_{max}: ultimate stress; ε_p: plastic strain. Reprinted from (Louzguine-Luzgin *et al.* 2005)

Alloy	HV	σ_y (MPa)	σ_{max} (MPa)	ε_p (%)	ρ (g/mm^3)	Phase constituents
$Ti_{65}Fe_{35}$	550	1800	2220	6.7	5.796	β-Ti, FeTi
$Ti_{68}Fe_{27}Co_5$	590	1765	1920	4.5	5.684	β-Ti, (Fe,Co)Ti
$Ti_{70}Fe_{20}Co_{10}$	560	1770	1890	8.1	5.669	β-Ti, (Fe,Co)Ti
$Ti_{76}Fe_{12}Co_{12}$	520	1640	1690	2.3	5.355	β-Ti, FeTi, Ti_2Co
$Ti_{73}Fe_{13.5}Co_{13.5}$	570	1860	1875	8	5.453	β-Ti, (Fe,Co)Ti
$Ti_{70}Fe_{15}Co_{15}$	540	1750	2350	16.5	5.601	β-Ti, (Fe,Co)Ti
$Ti_{70}Fe_{17}Co_{13}$	530	1630	2035	15	5.592	β-Ti, (Fe,Co)Ti
$Ti_{66}Fe_{19}Co_{15}$	540	1595	2160	15.3	5.754	β-Ti, (Fe,Co)Ti
$Ti_{66}Fe_{17}Co_{17}$	540	1700	1935	16	5.783	β-Ti, (Fe,Co)Ti
$Ti_{60}Fe_{20}Co_{20}$	550	1510	2100	15	6.042	β-Ti, (Fe,Co)Ti
$Ti_{54}Fe_{23}Co_{23}$	580	905	905	0.5	6.27	β-Ti, FeTi, Ti_2Co
$Ti_{70}Fe_{10}Co_{20}$	660	1640	1640	1	5.562	β-Ti, FeTi, Ti_2Co
$Ti_{73}Co_{27}$	620	1650	1650	0.1	5.418	β-Ti, Ti_2Co, α-Ti

microstructure and mechanical properties of the hypereutectic Ti-Fe-Co ternary alloys (Louzguina-Luzgina *et al.* 2006, 2009). V and Cu reduce the plasticity of the Ti-Fe-Co alloys whilst B generally reduces both strength and ductility (Louzguina-Luzgina *et al.* 2006). However, a trace of B addition (0.5 at.%) increases mechanical strength up to 2470 MPa (Louzguina-Luzgina *et al.* 2009). Sn significantly enhances the plasticity by sacrificing strength. For example, the $Ti_{67}Fe_{14}Co_{14}Sn_5$ alloy exhibited a high ultimate compressive strength of 1830 MPa and a large plastic strain of 24% (Louzguina-Luzgina *et al.* 2006). The alloying of Ni or Si leads to a drastic embrittlement of the samples (without distinct plastic deformation) (Louzguina-Luzgina *et al.* 2006, 2009).

Zhang *et al.* (2007a) investigated the effect of Sn on the microstructure, mechanical properties and deformation behaviour of the hypereutectic $Ti_{65}Fe_{35}$ binary alloy. All $(Ti_{0.65}Fe_{0.35})_{100-x}Sn_x$ ($x = 0$, 2.5 and 5%) alloys display considerable work hardening, high strength and large plasticity. The obtained mechanical properties are summarized in Table 1. As seen from Table 1, the addition of 2.5% Sn causes a significant increase in fracture strength by ~300 MPa and a noticeable enhancement of plasticity by ~5%. Further addition of Sn to 5% leads to a slight decrease in strength and in plasticity compared to the $Ti_{63.375}Fe_{34.125}Sn_{2.5}$ alloy. However, 5% Sn addition still toughens $Ti_{65}Fe_{35}$ alloy by enhancing the plasticity as well as maintaining a high strength. Therefore, a suitable Sn concentration could both improve the strength and enhance the plasticity of $Ti_{65}Fe_{35}$ alloy.

Fig. 2 shows the microstructure of the hypereutectic Ti-Fe-Sn alloys. The $Ti_{65}Fe_{35}$ (Fig. 2(a)) and $Ti_{63.375}Fe_{34.125}Sn_{2.5}$ (Fig. 2(b)) display a typical hypereutectic microstructure, where micrometer-sized FeTi primary dendrites are homogenously dispersed in an ultrafine-grained matrix. An example of TEM micrograph (Fig. 2(d)) reveals that the ultrafine eutectic matrix is composed of plate-shape FeTi (bright) and β-Ti (gray) phases. The 2.5% Sn addition to the $Ti_{65}Fe_{35}$ alloy slightly decreases

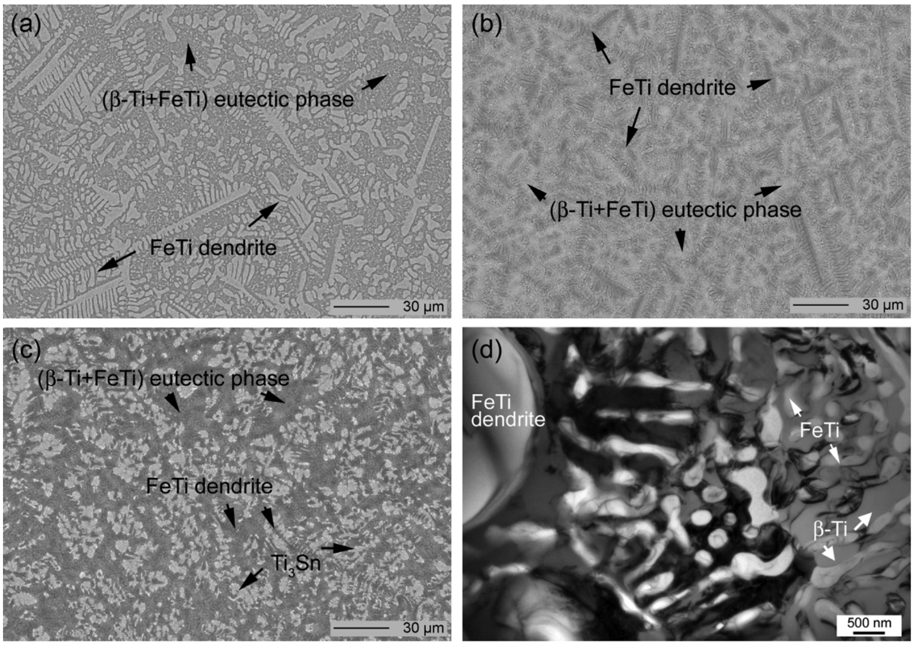

Fig. 2 SEM backscattered electron images of the overall microstructure for the $(Ti_{0.65}Fe_{0.35})_{100-x}Sn_x$ 3 mmØ rods showing primary micrometer-sized dendritic phase embedded in ultrafine-grained matrix: (a) x = 0, (b) x = 2.5 and (c) x = 5, and (d) bright-field TEM image of the $Ti_{63.375}Fe_{34.125}Sn_{2.5}$. Reprinted from (Zhang *et al.* 2007a, Zhang *et al.* 2010)

the sizes of the primary FeTi dendrites but significantly refines the grain size of the eutectic matrix in the $Ti_{65}Fe_{35}$ alloy (Fig. 2(b)). The width of the FeTi lamellae decreases from ~400 nm in $Ti_{65}Fe_{35}$ alloy to ~200 nm in the $Ti_{63.375}Fe_{34.125}Sn_{2.5}$ and that of β-Ti lamellae decreases from ~2.5 μm ($Ti_{65}Fe_{35}$) to ~160 nm ($Ti_{63.375}Fe_{34.125}Sn_{2.5}$). The volume fraction of the ultrafine (β-Ti + FeTi) eutectic in the bimodal composites increases from ~65% in $Ti_{65}Fe_{35}$ to ~72% in $Ti_{63.375}Fe_{34.125}Sn_{2.5}$. Energy-dispersive X-ray spectroscopy (EDS) analysis indicates that most Sn dissolves in the eutectic matrix in case of $Ti_{63.375}Fe_{34.125}Sn_{2.5}$, which could toughen the alloy due to solid solution hardening effect. This result is consistent with the X-ray diffraction (XRD) results that the Sn addition only changes the lattice parameter of β-Ti ($\alpha_{\beta\text{-Ti}}$) but the lattice parameter of FeTi remains unchanged (0.2991 nm). As a result, the 2.5% Sn addition in $Ti_{65}Fe_{35}$ alloy leads to the refinement of microstructure constituents (slightly smaller primary FeTi dendrites and significantly finer eutectic matrix, more than 10 times finer β-Ti solid solution phase) and an increase in the volume fraction of the ductile ultrafine-grained eutectic matrix by ~7 vol.%, resulting in the improvement of strength and plasticity in $Ti_{63.375}Fe_{34.125}Sn_{2.5}$. When the Sn content is raised to 5% (Fig. 2(c)), the alloy is composed of Ti_3Sn (bright), FeTi (gray) and (β-Ti + FeTi) eutectic phase. However, the $Ti_{61.75}Fe_{33.25}Sn_5$ alloy has a similar grain size of the FeTi dendrites and lamellar spacing of the eutectic as the $Ti_{63.375}Fe_{34.125}Sn_{2.5}$. The mean grain size of Ti_3Sn is about 10 μm. Accordingly, the Ti-Fe-Sn ultrafine hypereutectic composites have different phase structure, refinement and volume fractions of the constituent phases due to different Sn content, which may play important role on the mechanical properties (i.e., strength and plasticity) of the ultrafine composites.

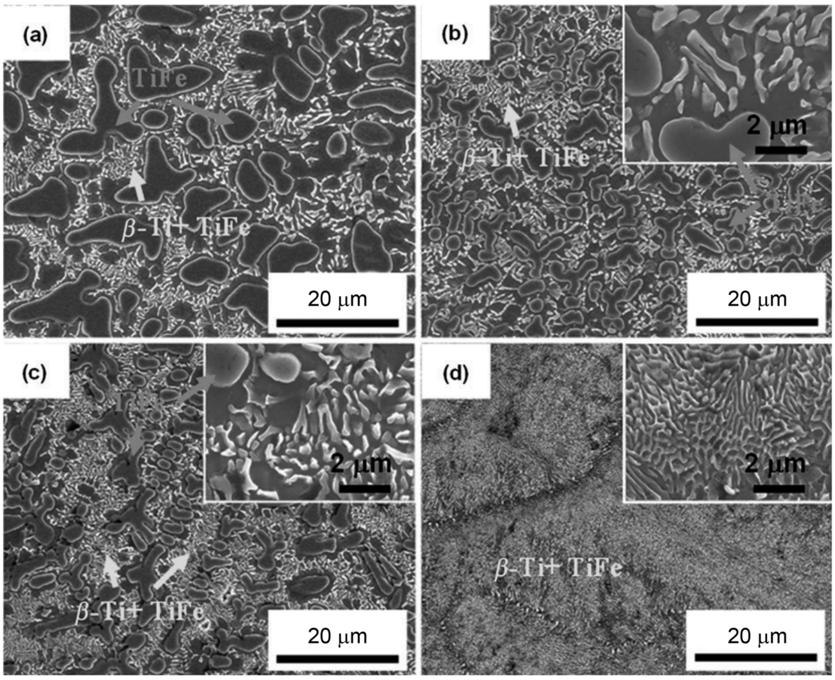

Fig. 3 SEM secondary electron micrographs of as-cast $(Ti_{0.655}Fe_{0.345})_{100-x}Nb_x$ alloys: (a) x = 0, (b) x = 3, (c) x = 5 and (d) x = 7. Reprinted from (Park *et al.* 2009)

The addition of Nb (Park *et al.* 2009) or Ga (Misra *et al.* 2010b) were also found to enhance the mechanical properties of the hypereutectic $Ti_{65}Fe_{35}$ alloy by the manipulation of the eutectic microstructure. Interestingly, 5% Nb addition ($(Ti_{0.655}Fe_{0.345})_{95}Nb_5$) significantly refine both primary FeTi and eutectic phases. Further increasing the Nb concentration to 7% ($(Ti_{0.655}Fe_{0.345})_{93}Nb_7$) resulted in a homogeneous ultrafine eutectic alloy without micron-scale dendrites, exhibiting the highest strength (~2600 MPa) combined with a large plasticity (~12%). The microstructure evolution with Nb concentration in the Ti-Fe-Nb alloys is shown in Fig. 3. These findings suggested that the improved deformation behavior of the ultrafine eutectic composites is closely related to suitable tuning of the microstructural features and the stability of the constituent phases.

2.3 Pseudo-eutectic bimodal composites

It was reported that the addition of 3.85% Sn in eutectic $Ti_{70.5}Fe_{29.5}$ alloy remains a homogenous ultrafine eutectic microstructure. The 3.85% Sn addition slightly decreases the strength but considerably enhances the compressive plasticity from 2.1% to 9.6% strain (Das *et al.* 2005). Further increasing the Sn concentration (4-6%) caused the precipitation of Ti_3Sn, as seen in Fig. 4, forming a bimodal composites with micrometer-sized Ti_3Sn embedded in a ultrafine (β-Ti + FeTi) eutectic matrix (Das *et al.* 2010). Continuous increasing the Sn content further enhanced the microstructural heterogeneities, forming a coarse (β-Ti + Ti_3Sn) eutectic as well as a fine (β-Ti + FeTi) eutectic, as seen in Fig. 5 (Han *et al.* 2008). The difference in the length scale of the lamellar

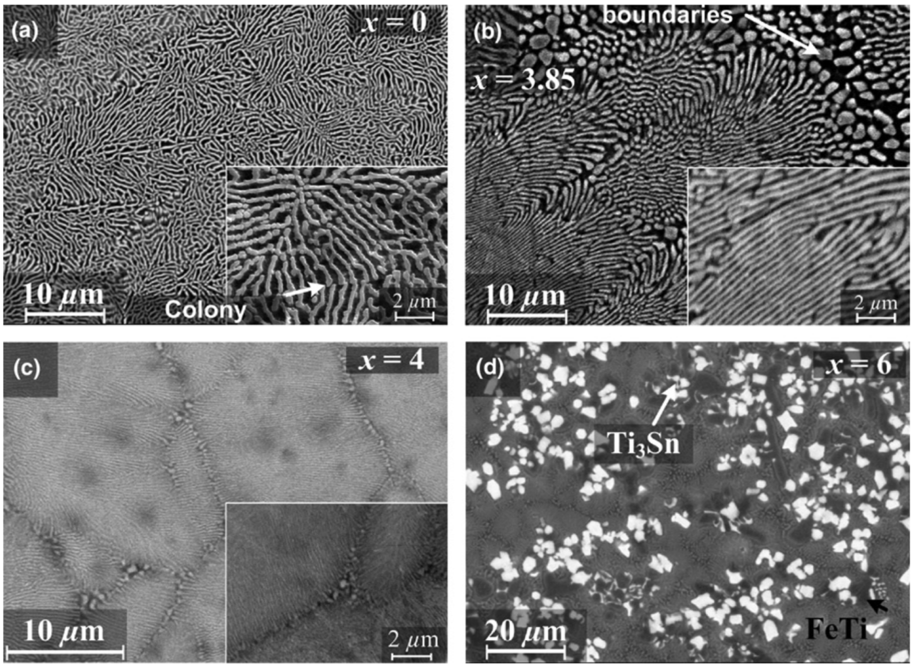

Fig. 4 SEM backscattered electron images of $(Ti_{0.705}Fe_{0.295})_{100-x}Sn_x$ 6 mmØ rods showing a homogenous ultrafine eutectic microstructure: (a) x = 0, (b) x = 3.85, (c) x = 4, and (d) pro-eutectic Ti_3Sn forms in x = 6. Insets show the refinement and modification of the colony boundaries. Reprinted from (Das *et al.* 2010)

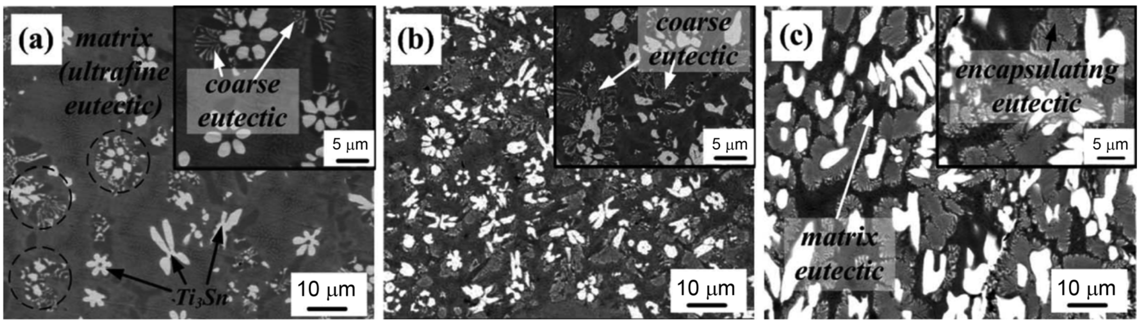

Fig. 5 SEM backscattering electron micrographs of as-cast $(Ti_{0.705}Fe_{0.295})_{100-x}Sn_x$ alloys with (a) x = 5, (b) x = 7, and (c) x = 9, showing the formation of heterogeneous ultrafine pseudo-eutectic microstructure. Reprinted from (Han *et al.* 2008)

spacing between the (β-Ti + Ti_3Sn) and (FeTi + β-Ti) eutectics originates form the large difference in the eutectic temperature and the diffusion coefficient of the constituent elements. The microstructural heterogeneities in these ultrafine eutectic bimodal composites significantly enhance the compressive plasticity up to ~15.7%. The additions of In and/or Nb to the binary eutectic alloy significantly modified the microstructure from eutectic microstructure to a dendrite-eutectic microstructure, resulting in the improvement in both strength from 1926 MPa for the $Ti_{70.5}Fe_{29.5}$ to

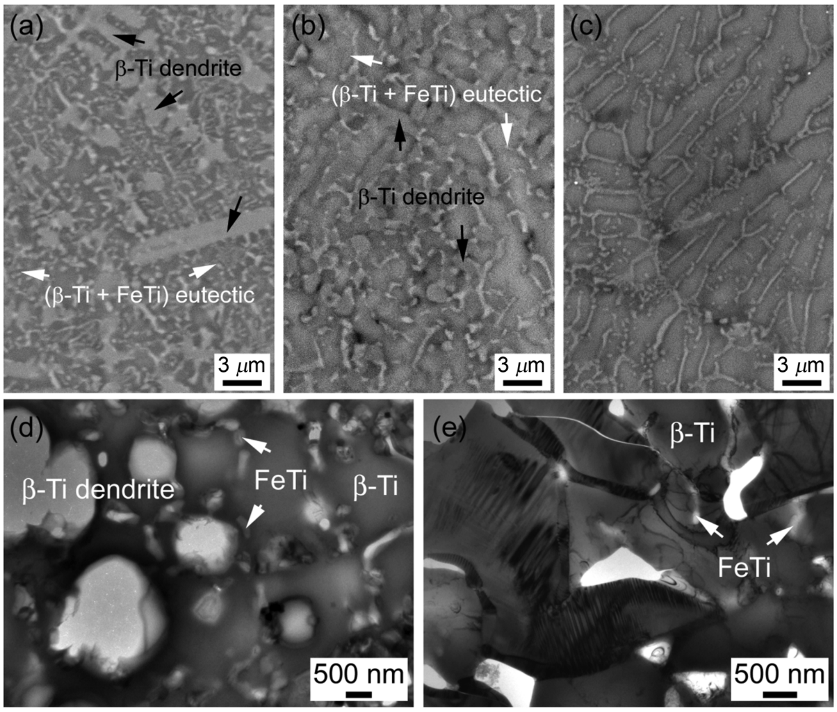

Fig. 6 Microstructures of the as-cast $(Ti_{0.72}Fe_{0.28})_{100\text{-}x}Ta_x$ 3 mmØ rods. SEM backscattered electron images of (a) x = 0 and (b) x = 2 showing a hypoeutectic microstructure with micrometer-sized primary β-Ti dendritic phase embedded in an ultrafine-grained (β-Ti + FeTi) matrix, and (c) x = 4 showing a carcass (pseudo-hypoeutectic) microstructure. Microstructural details were confirmed by bright-filed TEM micrographs of (d) x = 0 and (e) x = 4

2498 MPa for the $Ti_{66}Fe_{27.5}In_{3.5}Nb_3$ and plasticity from 0.6% plastic strain for the $Ti_{70.5}Fe_{29.5}$ to 3.6% for the $Ti_{66}Fe_{27.5}In_{3.5}Nb_3$ (Misra *et al.* 2010a).

2.4 Hypoeutectic bimodal composites

Limited work has been conducted on the hypoeutectic bimodal microstructure with respect to the hypereutectic and (pseudo-)eutectic bimodal composites (Louzguine-Luzgin *et al.* 2005, Louzguine-Luzgin *et al.* 2007, Zhang *et al.* 2007b). This section gives an example of the microstructure and mechanical properties of the as-cast $(Ti_{0.72}Fe_{0.28})_{100\text{-}x}Ta_x$ (x = 0, 2 and 4%) 3 mmØ rods.

XRD results reveal that all alloys mainly consist of β-Ti and FeTi solid solutions. The Ta addition altered the lattice parameters of both β-Ti and FeTi. This is quite different from the scenario in all aforementioned ultrafine-grained Ti-Fe-based bimodal alloys, where there is no change in the lattice parameter of FeTi phase. Furthermore, the increase of the Ta concentration led to a higher lattice strain in β-Ti phase. Both the $Ti_{72}Fe_{28}$ (Fig. 6(a)) and $Ti_{70.56}Fe_{27.44}Ta_2$ (Fig. 6(b)) alloys show a hypoeutectic microstructure, where micrometer-sized β-Ti primary dendrites (indicated by black arrows) are embedded in an ultrafine-grained (β-Ti + FeTi) eutectic matrix (denoted by white arrows). The 2% Ta slightly modified the grain size of β-Ti primary dendrites, but significantly coarsened (~3 times) the β-Ti and FeTi lamellae in the eutectic. The $Ti_{69.12}Fe_{26.88}Ta_4$ alloy (Fig. 6(c)) has a carcass microstructure (pseudo-hypoeutectic) composed of ultrafine FeTi (~250 nm) and micrometer-sized β-Ti (~1.2 μm) solid solutions. TEM observations confirmed that both $Ti_{72}Fe_{28}$ and $Ti_{70.56}Fe_{27.44}Ta_2$ are composed of micrometer-sized β-Ti primary dendrites embedded in an ultrafine-grained (β-Ti + FeTi) eutectic matrix (Fig. 6(d)). $Ti_{69.12}Fe_{26.88}Ta_4$ consists of nanoscale twins along with the β-Ti and FeTi phases (Fig. 6(e)). However, the selected area electron diffraction (SAED) patterns (Zhang *et al.* 2010) revealed that the $Ti_{72}Fe_{28}$ and $Ti_{70.56}Fe_{27.44}Ta_2$ alloys show different structural features in the matrix, where ω-Ti-like phase presents in the matrix of $Ti_{70.56}Fe_{27.44}Ta_2$ but disappear in the matrix of $Ti_{72}Fe_{28}$.

The mechanical properties of the Ti-Fe-Ta alloys are given in Table 1. All three alloys show high yield strength in excess of 2000 MPa, high fracture strength exceeding 2500 MPa, and large plasticity. The changes in the mechanical properties should be ascribed to the structural modulation with the Ta addition. The appearance of ω-Ti-like phase and 0.24% higher lattice strain in β-Ti phase in the $Ti_{70.56}Fe_{27.44}Ta_2$ alloy will increases the dislocation pileup stress and decreases the intrinsic cleavage strength (Lazar *et al.* 2005), reducing the plasticity of 7.5% in the $Ti_{72}Fe_{28}$ alloy to 1.0% in $Ti_{70.56}Fe_{27.44}Ta_2$ alloy (Table 1). On the other hand, the presence of nanoscale twins in the $Ti_{69.12}Fe_{26.88}Ta_4$ may facilitate the dislocation slip and enhance the plasticity. Therefore, the $Ti_{69.12}Fe_{26.88}Ta_4$ alloy regains a large plasticity (Zhang *et al.* 2007b).

3. Mechanical properties

Advanced metallic materials, such as nanostructured / ultrafine-grained metals and alloys and bulk metallic glasses (BMGs), are well known to have several times higher strength than their conventional coarse-grained counterparts. Ti-based BMGs and BMG matrix composites (Zhang and Inoue 2001, Zhang *et al.* 2002, 2006b, Zhang and Xu 2002, Ma *et al.* 2004, Guo *et al.* 2005, Zhang *et al.* 2005, Zhang *et al.* 2006a, Calin *et al.* 2007, Huang *et al.* 2007, Oak *et al.* 2007, Ohkuboa *et al.* 2007, Hofmann *et al.* 2008, Wang *et al.* 2008, Zheng *et al.* 2010) often exhibit a high fracture strength exceeding ~2000 MPa but very limited plasticity (<0.5%). Some Ti-based BMGs also exhibit a larger plasticity of 1-11%. However, the plasticity of these Ti-based BMGs does not result from the glassy phase itself. Detailed microstructural observations confirmed that these Ti-based BMGs have a nanocrystals / BMG matrix composite microstructure and their plasticity is strongly linked to the amount of nanocrystals embedded in glassy matrix (Ohkuboa *et al.* 2007). Ti-based BMG matrix composites show large plasticity through sacrificing the strength by about 300-500 MPa. The current Ti-based ultrafine-grained alloys with multiple length-scale phases were developed in a very similar manner to BMG matrix composites. The significant difference between BMGs and bimodal composites is that the continuous matrix material is comprised of an ultrafine-grained eutectic in bimodal composites instead of a metallic glass phase in BMGs. Nevertheless, the ultrafine-grained alloys with multiple length-scale phases exhibit a large plasticity without significant sacrificing the strength. Fig. 7 compares the mechanical properties of the as-cast ultrafine-grained titanium bimodal composites with the commercial titanium alloy (e.g., Ti-6Al-4V grade 5 STA), Ti-based BMGs (Zhang and Inoue 2001, Ma *et al.* 2004, Huang *et al.* 2007, Oak *et al.* 2007) and Ti-based BMG matrix composites (Hofmann *et al.* 2008). Apparently, the ultrafine-grained titanium alloys with multiple length-scale phases exhibit better mechanical properties (in terms of yield strength, ultimate strength and plasticity) than the Ti-based BMGs and BMG matrix

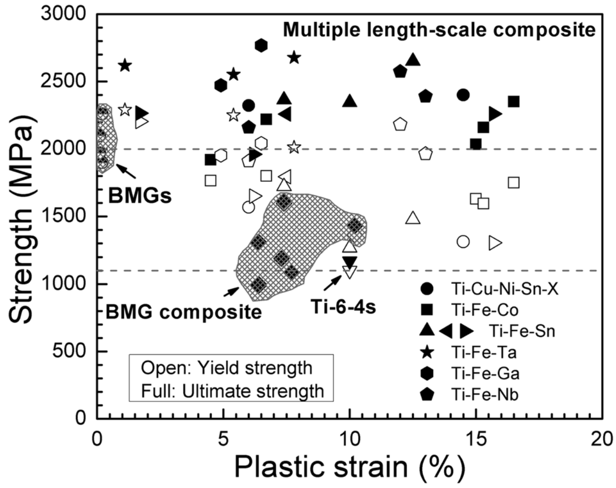

Fig. 7 Comparison of the mechanical properties of the nanostructured / ultrafine-grained Ti-Fe-based alloys with multiple length-scale phases with some Ti-based bulk metallic glasses (Zhang and Inoue 2001, Ma *et al.* 2004, Huang *et al.* 2007, Oak *et al.* 2007, Wang *et al.* 2008) and bulk metallic glasses composites (Hofmann *et al.* 2008) as well as the commercial Ti-6Al-4V alloy

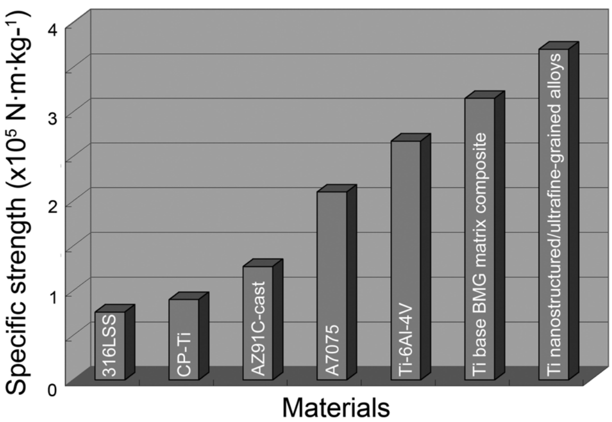

Fig. 8 Specific strength of nanostructured / ultrafine-grained titanium alloys with multiple length-scale phases compared with other titanium alloys as well as selected commercial engineering structural materials

composites. Increasing the plasticity / strength of metals without sacrificing other properties (strength, plasticity, etc.) is a critical issue in the alloy development, as they are competitiveness. Therefore, by proper selection of constituent phases and introducing multiple length scales into microstructure may provide a possible route to enhance the plasticity without significant sacrificing the strength of nanostructured / ultrafine-grained eutectic composites.

Fig. 8 compares the specific fracture strength of nanostructured / ultrafine-grained titanium bimodal composites with Ti-based BMG matrix composites and other commercial engineering structural materials. The extremely high specific strength values in the titanium based nanostructured / ultrafine-grained alloys with multiple length-scale phases and Ti-based BMG matrix composites, as two advanced high-strength titanium alloys, are particularly attractive. Note that, nanostructured / ultrafine-grained titanium alloys with multiple length-scale phases show a higher specific strength than the Ti-based BMG matrix composites. These nanostructured / ultrafine-grained titanium bimodal composites have ~1.5 times higher specific strength than the Ti-6Al-4V. Therefore, the combination of high strength and high specific strength as well as large plasticity of the nanostructured / ultrafine-grained titanium alloys with multiple length-scale phases may create opportunities in the potential applications requiring high strength.

4. Deformation mechanism

As described in Section 2, most bimodal composites have two or more phase constituents, i.e., micronmeter-sized primary phase (dendrite or eutectic) and ultrafine eutectic, despite their hypereutectic, pseudo-eutectic or hypoeutectic microstructure. The deformation mechanism of the nanostructured / ultrafine-grained titanium bimodal composites might be revealed by investigation of the microstructure-properties relationship as well as the fracture morphology in these alloys.

A number of work has detailed investigated the grain size / lamellar spacing and volume fraction of constituent phases (i.e., primary dendrites or eutectic) in the microstructure (Zhang *et al.* 2007a, Zhang *et al.* 2007b, 2010, Park *et al.* 2009, Das *et al.* 2010). These structural features play a basic role on the mechanical properties in the nanostructured / ultrafine-grained titanium bimodal composites. In the case of the hypereutectic $(Ti_{0.65}Fe_{0.35})_{100-x}Sn_x$ bimodal composites, the 2.5% Sn addition to the $Ti_{65}Fe_{35}$ alloy significantly refines the lamellar spacing of the eutectic matrix (i.e., the spacing of β-Ti and FeTi decreased from ~2.5 μm and 400 nm for x = 0 to 160 nm and 200 nm for x = 2.5, respectively) along with increase ~7% higher fraction of ultrafine eutectic (Zhang *et al.* 2007a). For the hypoeutectic $(Ti_{0.72}Fe_{0.28})_{100-x}Ta_x$ alloys, the 2% Ta led to ~3 times coarser eutectic lamellae as well as a lower volume fraction of the ultrafine eutectic when compared with the $Ti_{72}Fe_{28}$ (Zhang *et al.* 2007b). Therefore, in spite of the same phase constituents in microstructure, a finer grain size/lamellar spacing and/or higher volume fraction of ultrafine eutectic in microstructure could result in a higher strength together with a larger plasticity. Therefore, the enhancement of the mechanical properties are mainly owing to the synergistic effect of the supersaturating of the β-Ti solid solution phase (solid solution hardening effect) and the refinement of the constituent phases (Hall-Petch effect) as well as the volume fraction of the phase constituents. As result, the microstructural feature of the phase constituents, such as their volume fraction, morphology, and size, is responsible for the overall deformation behavior.

Fig. 9 displays an example of the fracture morphology of the hypereutectic $(Ti_{0.65}Fe_{0.35})_{100-x}Sn_x$ alloys. All fracture morphologies mainly consists of cleavage fracture along with a few elongated dimples. The cleavage planes of the FeTi dendrites make multiple steps on the fracture surface displaying river-like patterns, as denoted by the arrows. The morphology of the river-like patterns is somewhat different due to the size and volume fraction of the primary dendrites. An enlarged view of the fracture morphology of the primary FeTi dendrites (cleavage) and the eutectic matrix (dimple) is shown in Fig. 9(d). Interestingly, a blockage of slip bands, which were formed in the (β-Ti + FeTi) eutectic, by the primary FeTi dendrites at the dendrite/eutectic interface under compression can be observed on the fracture surface (Fig. 9 inset). This is presumably due to the relatively higher hardness of the primary FeTi dendrites compared to the (β-Ti + FeTi) eutectic. It is noted that cracks, as indicated by white arrows, are apparent around the Ti_3Sn phase in the failed

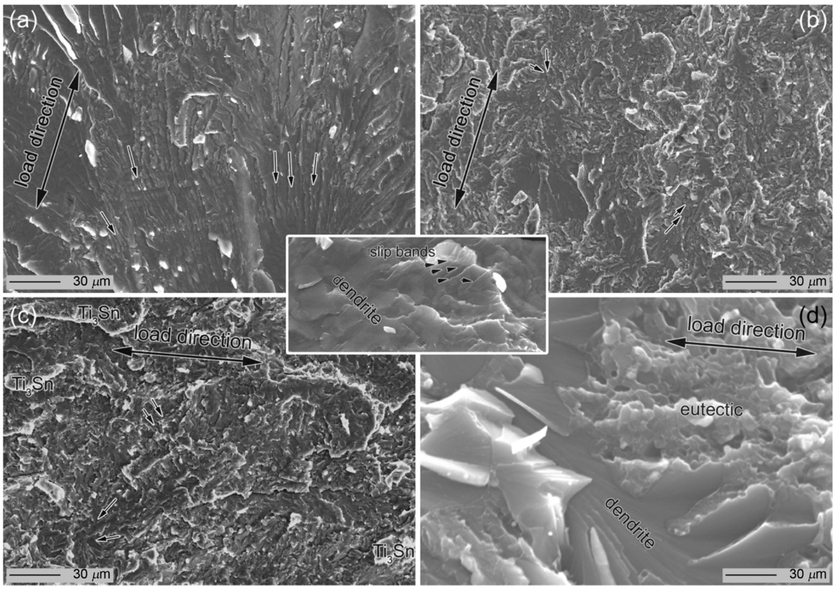

Fig. 9 SEM secondary electron images of the fractured surfaces for the $(Ti_{0.65}Fe_{0.35})_{100\text{-}x}Sn_x$ rods: (a) x = 0, (b) x = 2.5, (c) x = 5 and (d) an enlarged view of the fracture morphology of the primary FeTi dendrites and the eutectic matrix. The inset shows the blockage of slip bands formed in the eutectic matrix at the dendrite/eutectic interface. Reprinted from (Zhang *et al.* 2007a)

$Ti_{61.75}Fe_{33.25}Sn_5$ (Fig. 9(c)). This is related to the structural incompatibility between hexagonal Ti_3Sn ($D0_{19}$) and b.c.c. FeTi (B2) and β-Ti (A2), which blocks the dislocation transfer across their interfaces, accelerates the failure around Ti_3Sn phase (Zhang *et al.* 2007a). Both A2 and B2 phases have the same main slip systems ($\frac{1}{3}\langle\bar{1}11\rangle\{100\}$,$\frac{1}{2}\langle\bar{1}11\rangle\{211\}$ and $\frac{1}{2}\langle\bar{1}11\rangle\{321\}$), while the $D0_{19}$ phase has different main slip systems (prism $\frac{1}{3}\langle 1\bar{2}10\rangle\{10\bar{1}0\}$, basal $\frac{1}{3}\langle 1\bar{2}10\rangle\{0001\}$ and pyramidal $\frac{1}{3}\langle 11\bar{2}\bar{6}\rangle\{1121\}$). The compatibility between the A2 and B2 structures will enhance the plasticity by slip transfer to relieve dislocation pile-ups at the A2/B2 interface. In contrast, the mismatch of the structure between $D0_{19}$ and A2 and B2 will make the dislocation transfer across the $D0_{19}$/A2 and/or $D0_{19}$/B2 interfaces difficult, resulting in cracks around the $D0_{19}$ phase and inducing relatively early fracture, as shown the failure around Ti_3Sn phase in Fig. 9(c). Therefore, compatible structure between phase constituents might contribute to the improvement of the mechanical properties.

Furthermore, it is reported that the change in the lattice parameter of the β-Ti phase in eutectic and their intrinsic elastic properties as well as the short-range order of the eutectic β-Ti phase are also associated with the improvement of plasticity (Louzguine *et al.* 2004, Zhang *et al.* 2007b, Park *et al.* 2009, Das *et al.* 2010). It is suggested that the addition of Sn or Nb to Ti-Fe alloy is effective to introduce a spatial heterogeneity at the interfacial areas, thus minimizing the interfacial strain between the β-Ti solid solution and the FeTi compound (Louzguine *et al.* 2004, Park *et al.* 2009). In most the aforementioned studies in Ti-Fe alloy systems, the alloying of additional elements (i.e., Sn, Co, Nb) cause a quite large lattice mismatch between the β-Ti and FeTi phases, as revealed by the increase in the lattice parameter of β-Ti (Zhang *et al.* 2007a, Park *et al.* 2009), and simultaneously introduce a coherency strain as well as minimizes the coherency stress at the interface, which may be favorable to absorb dislocations from the β-Ti phase. A large number of shears interaction / blockage in hypereutectic Ti-Fe-Sn and Ti-Fe-Nb samples suggested that the deformation behavior is improved in terms of branching and multiplication of principle shear bands, together with a homogeneous distribution of numerous fine shear bands (Park *et al.* 2009).

5. Conclusions

Ultrafine-grained titanium alloys with multiple length-scale phases have been developed by simple one-step processing. The as-prepared titanium bimodal composites exhibit high strength exceeding 2000 MPa and enhanced plasticity of up to 15-20%, as well as high specific strength. The enhanced mechanical properties result from the introducing multiple length scales in microstructure, suggesting this strategy is a promising route to enhance plasticity without sacrificing high strength. The interface between eutectic structures acts as a nucleation site for shear bands and different eutectic structure effectively inhibits the propagation of shear bands. The deformation mechanism is strongly linked to the nanostructured / ultrafine-grained eutectic matrix by nucleation, pinning and multiplication of shear bands during deformation. The mechanical properties and deformation behaviour of the nanostructured / ultrafine-grained Ti-Fe-based alloys with multiple length-scale phases are determined by the synergistic effects of: (i) the morphology, refinement and the volume fraction of the phase constituents, (ii) the compatibility of the phase structures, and (iii) the structural short-range order and the lattice strain of the β phase. Accordingly, it is very important to tailor the microstructural features of these bimodal composites by proper selection of micro-alloying elements base on the structure point of view and controlling of the solidification process. The nanostructured / ultrafine-grained titanium alloys with multiple length-scale phases demonstrate competitive mechanical properties than conventional titanium alloys and other high-strength titanium alloys, which creates some potential applications requiring high strength.

Acknowledgements

The author thanks J. Eckert, H.B. Lu, M. Calin, C. Duhamel, J. Das, K.B. Kim, J. Xu, E. Ma and U. Kühn for stimulating discussions, and M. Frey, H.J. Klauß, S. Donath and C. Mickel for technical assistance. The author is also very grateful for the financial support of the Alexander von Humboldt Foundation and the UWA Research Development Award.

References

Calin, M., Zhang, L.C. and Eckert, J. (2007), “Tailoring of microstructure and mechanical properties of a Ti-based bulk metallic glass-forming alloy”, *Scripta Mater.,* **57**(12), 1101-1104.

Das, J., Kim, K.B., Baier, F., Loser, W. and Eckert, J. (2005), “High-strength Ti-base ultrafine eutectic with enhanced ductility”, *Appl. Phys. Lett.,* **87**(16), 161907.

Das, J., Theissmann, R., Loser, W. and Eckert, J. (2010), “Effect of Sn on microstructure and mechanical properties of Ti-Fe-(Sn) ultrafine eutectic composites”, *J. Mater. Res.,* **25**(5), 943-956.

Guo, F.Q., Wang, H.J., Poon, S.J. and Shiflet, G.J. (2005), “Ductile titanium-based glassy alloy ingots”, *Appl. Phys. Lett.,* **86**(9), 091907.

Han, J.H., Kim, K.B., Yi, S., Park, J.M., Sohn, S.W., Kim, T.E., Kim, D.H., Das, J. and Eckert, J. (2008),

"Formation of a bimodal eutectic structure in Ti-Fe-Sn alloys with enhanced plasticity", *Appl. Phys. Lett.,* **93**(14), 141901.
He, G., Eckert, J., Loser, W. and Schultz, L. (2003), "Novel Ti-base nanostructure-dendrite composite with enhanced plasticity", *Nature Mater.,* **2**(1), 33-37.
Hofmann, D.C., Suh, J.Y., Wiest, A., Lind, M.L., Demetriou, M.D. and Johnson, W.L. (2008), "Development of tough, low-density titanium-based bulk metallic glass matrix composites with tensile ductility", *P. Natl. Acad. Sci. USA,* **105**(51), 20136-20140.
Huang, Y.J., Shen, J., Sun, J.F. and Yu, X.B. (2007), "A new Ti-Zr-Hf-Cu-Ni-Si-Sn bulk amorphous alloy with high glass-forming ability", *J. Alloy. Compd.,* **427**(1-2), 171-175.
Inoue, A. (2000), "Stabilization of metallic supercooled liquid and bulk amorphous alloys", *Acta Mater.,* **48**(1), 279-306.
Johnson, W.L. (1999), "Bulk glass-forming metallic alloys: Science and technology", *MRS Bull.,* **24**(10), 42-56.
Koch, C.C. (2003), "Ductility in nanostructured and ultra fine-grained materials: recent evidence for Optimism", *J. Metast. Nano. Mater.*, **18**, 9-20.
Lazar, P., Podloucky, R. and Wolf, W. (2005), "Correlating elasticity and cleavage", *Appl. Phys. Lett.,* **87**(26), 261910.
Louzguina-Luzgina, L.V., Louzguine-Luzgin, D.V. and Inoue, A. (2006), "Influences of additional alloying elements (V, Ni, Cu, Sn, B) on structure and mechanical properties of high-strength hypereutectic Ti-Fe-Co bulk alloys", *Intermetallics,* **14**(3), 255-259.
Louzguina-Luzgina, L.V., Louzguine-Luzgin, D.V. and Inoue, A. (2009), "Effect of B addition to hypereutectic Ti-based alloys", *J. Alloy. Compd.,* **474**(1-2), 131-133.
Louzguina, L.V., Louzguine-Luzgin, D.V. and Inoue, A. (2005), "Ultra-strong and ductile hypereutectic Ti-based bulk alloys", *J. Metastable Nanocryst. Mater,* **24-25**, 265-268.
Louzguine-Luzgin, D.V., Louzguina-Luzgina, L.V., Kato, H. and Inoue, A. (2005), "Investigation of Ti-Fe-Co bulk alloys with high strength and enhanced ductility", *Acta Mater.,* **53**(7), 2009-2017.
Louzguine-Luzgin, D.V., Louzguina-Luzgina, L.V. and Inoue, A. (2007), "Deformation behavior of high strength metastable hypereutectic Ti-Fe-Co alloys", *Intermetallics,* **15**(2), 181-186.
Louzguine, D.V., Kato, H., Louzguina, L.V. and Inoue, A. (2004), "High-strength binary Ti-Fe bulk alloys with enhanced ductility", *J. Mater. Res.,* **19**(12), 3600-3606.
Ma, C.L., Ishihara, S., Soejima, H. Nishiyama, N. and Inoue, A. (2004), "Formation of new Ti-based metallic glassy alloys", *Mater. Trans.,* **45**(5), 1802-1806.
Ma, E. (2003a), "Nanocrystalline materials: Controlling plastic instability", *Nature Mater.,* **2**(1), 7-8.
Ma, E. (2003b), "Instabilities and ductility of nanocrystalline and ultrafine-grained metals", *Scripta Mater.,* **49**(7), 663-668.
Ma, E. (2006), "Eight routes to improve the tensile ductility of bulk nanostructured metals and alloys", *JOM,* **58**(4), 49-53.
Misra, D.K., Sohn, S.W., Gabrisch, H. Kim, W.T. and Kim, D.H. (2010a), "High strength Ti-Fe-(In, Nb) composites with improved plasticity", *Intermetallics,* **18**(3), 342-347.
Misra, D.K., Sohn, S.W., Kim, W.T. and Kim. D.H. (2010b), "High strength hypereutectic Ti-Fe-Ga composites with improved plasticity", *Intermetallics,* **18**(2), 254-258.
Oak, J.J., Louzguine-Luzgin, D.V. and Inoue, A. (2007), "Fabrication of Ni-free Ti-based bulk-metallic glassy alloy having potential for application as biomaterial, and investigation of its mechanical properties, corrosion, and crystallization behavior", *J. Mater. Res.,* **22**(5), 1346-1353.
Ohkuboa, T., Nagahamaa, D., Mukaia, T. and Hono, K. (2007), "Stress–strain behaviors of Ti-based bulk metallic glass and their nanostructures", *J. Mater. Res.,* **22**(5), 1406-1413.
Park, J.M., Han, J.H., Kim, K.B. Mattern, N., Eckert, J. and Kim, D.H. (2009), "Favorable microstructural modulation and enhancement of mechanical properties of Ti-Fe-Nb ultrafine composites", *Philos. Mag. Lett.,* **89**(10), 623-632.
Song, G.A., Han, J.H., Kim, T.E. Park, J.M., Kim, D.H., Yi, S., Seo, Y., Lee, N.S. and Kim, K.B. (2011), "Heterogeneous eutectic structure in Ti-Fe-Sn alloys", *Intermetallics,* **19**(4), 536-540.
Sun, B.B., Sui, M.L., Wang, Y.M., He, G., Eckert, J. and Ma, E. (2006), "Ultrafine composite microstructure in a bulk Ti alloy for high strength, strain hardening and tensile ductility", *Acta Mater.,* **54**(5), 1349-1357.

Wang, Y.L., Ma, E. and Xu, J. (2008), "Bulk metallic glass formation near the TiCu-TiNi pseudo-binary eutectic composition", *Philos. Mag. Lett.,* **88**(5), 319-325.
Wang, Y.M., Chen, M.W., Zhou, F.H. and Ma, E. (2002), "High tensile ductility in a nanostructured metal", *Nature,* **419**(6910), 912-915.
Zhang, L.C. and Xu, J. (2002), "Formation of glassy $Ti_{50}Cu_{20}Ni_{24}Si_4B_2$ alloy by high-energy ball milling", *Mater. Sci. Forum,* **386-388**, 47-52.
Zhang, L.C., Xu, J. and Ma, E. (2002), "Mechanically alloyed amorphous Ti50(Cu0.45Ni0.55)(44-*x*)Al*x*Si4B2 alloys with supercooled liquid region", *J. Mater. Res.,* **17**(7), 1743-1749.
Zhang, L.C., Shen, Z.Q. and Xu, J. (2005), "Thermal stability of mechanically alloyed boride/ Ti50Cu18Ni22Al4Sn6 glassy alloy composites", *J. Non-Cryst. Solids,* **351**(27-29), 2277-2286.
Zhang, L.C., Xu, J. and Eckert, J. (2006a), "Thermal stability and crystallization kinetics of mechanically alloyed TiC/Ti-based metallic glass matrix composite", *J. Appl. Phys.,* **100**(3), 033514.
Zhang, L.C., Xu, J. and Ma, E. (2006b), "Consolidation and properties of ball-milled Ti50Cu18Ni22Al4Sn6 glassy alloy by equal channel angular extrusion", *Mat. Sci. Eng. A,* **434**(1-2), 280-288.
Zhang, L.C., Das, J., Lu, H.B., Duhamel, C., Calin, M. and Eckert, J. (2007a), "High strength Ti-Fe-Sn ultrafine composites with large plasticity", *Scripta Mater.,* **57**(2), 101-104.
Zhang, L.C., Lu, H.B., Mickel, C. and Eckert, J. (2007b), "Ductile ultrafine-grained Ti-based alloys with high yield strength", *Appl. Phys. Lett.,* **91**(5), 051906.
Zhang, L.C., Lu, H.B., Calin, M. Pereloma, E.V. and Eckert, J. (2010), "High-strength ultrafine-grained Ti-Fe-Sn alloys with a bimodal structure", *J. Phys. Conf. Ser.,* **240**(1), 012103.
Zhang, L.C., Calin, M. and Eckert, J. (2011), "High-strength titanium base alloys with multiple length-scale microstructure", Chapter 8 in: David E. Malach (Ed.), *Advances in Mechanical Engineering Research,* Volume 2, Nova Science Publishers, ISBN 978-1-61761-984-7, Hauppauge, NY, USA.
Zhang, T. and Inoue, A. (2001), "Ti-based amorphous alloys with a large supercooled liquid region", *Mater. Sci. Eng. A-Struct.,* **304**(1-2), 771-774.
Zheng, N., Wang, G., Zhang, L.C., Calin, M., Stoica, M., Vaughan, G., Mattern, N. and Eckert, J. (2010), "In situ high-energy x-ray diffraction observation of structural evolution in a Ti-based bulk metallic glass upon heating", *J. Mater. Res.,* **25**(12), 2271-2277.